

**Ground-state properties of closed-shell nuclei with low-momentum realistic interactions**L. Coraggio,<sup>1</sup> N. Itaco,<sup>1</sup> A. Covello,<sup>1</sup> A. Gargano,<sup>1</sup> and T. T. S. Kuo<sup>2</sup><sup>1</sup>*Dipartimento di Scienze Fisiche, Università di Napoli Federico II, and Istituto Nazionale di Fisica Nucleare, Complesso Universitario di Monte S. Angelo, Via Cintia, I-80126 Napoli, Italy*<sup>2</sup>*Department of Physics, SUNY, Stony Brook, New York 11794, USA*

(Received 21 May 2003; published 22 September 2003)

Ground-state properties of  $^{16}\text{O}$  and  $^{40}\text{Ca}$  are calculated with a low-momentum nucleon-nucleon potential  $V_{\text{low-k}}$ , derived from the chiral next-to-next-to-next-to-leading-order interaction recently constructed by Entem and Machleidt. The smooth  $V_{\text{low-k}}$  is used directly in a Hartree-Fock approach, avoiding the difficulties of the Brueckner-Hartree-Fock procedure. Corrections up to third order in the Goldstone expansion are evaluated, leading to results that are in very good agreement with experiment. Convergence properties of the expansion are examined.

DOI: 10.1103/PhysRevC.68.034320

PACS number(s): 21.30.Fe, 21.60.Jz, 21.10.Dr

**I. INTRODUCTION**

A fundamental problem in nuclear theory has long been the calculation of the bulk properties of closed-shell nuclei, such as their binding energy and charge radius, starting from realistic nucleon-nucleon ( $NN$ ) potentials. Potentials such as CD-Bonn [1], Nijmegen [2], Argonne  $v_{18}$  [3], and the new chiral potential of Ref. [4] reproduce the  $NN$  scattering data and the observed deuteron properties very accurately, but, because of their strong repulsion at short distances, none of them can be used directly in nuclear structure calculations.

A traditional approach to this problem is the Brueckner-Goldstone (BG) theory [5], where the Goldstone perturbative expansion is reordered summing to all orders a selected class of diagrams, the ladder diagrams. This implies replacing the bare interaction ( $V_{NN}$ ) vertices by the reaction matrix ( $G$ ) ones and omitting the ladder diagrams. Within this framework, one has the well-known Brueckner-Hartree-Fock (BHF) theory when the self-consistent definition is adopted for the single-particle (SP) auxiliary potential and only the first-order contribution in the BG expansion is taken into account. The BHF approximation gives therefore a mean field description of the ground state of nuclei in terms of the  $G$  matrix, the latter taking into account the correlations between pairs of nucleons. However, owing to the energy dependence of  $G$ , this procedure is not without difficulties. An important issue is the choice of the SP energies for states above the Fermi surface, which are not uniquely defined [6].

Calculations for finite nuclei within the BHF approach lead usually to insufficient binding energy as well as too small charge radii [7]. In this context, extensions of the conventional BHF approach have been proposed to account for long-range correlations [8]. It is worth mentioning that alternative approaches have been developed, as for instance the correlated basis function method [9] and the coupled cluster method [10], in both of which correlations are directly embedded into the wave functions. A comprehensive review of the various methods is given in Ref. [11], which also includes a discussion of calculations for nuclear matter as well as for finite nuclei. Another effort in this direction is the unitary model-operator approach of Suzuki and Okamoto [12].

Recently, a new technique to renormalize the short-range repulsion of a realistic  $NN$  potential by integrating out its high-momentum components has been proposed [13,14]. The resulting low-momentum potential, which we call  $V_{\text{low-k}}$ , is a smooth potential that preserves the low-energy physics of  $V_{NN}$  and is therefore suitable for being used directly in nuclear structure calculations. We have employed  $V_{\text{low-k}}$  derived from modern  $NN$  potentials to calculate shell-model effective interactions by means of the  $\hat{Q}$ -box plus folded diagram method. Within this framework, several nuclei with few valence particles have been studied [15–17], leading to the conclusion that  $V_{\text{low-k}}$  is a valid input for realistic shell-model calculations.

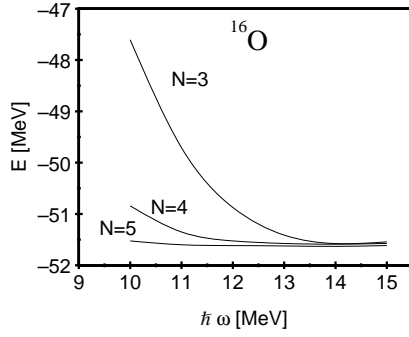
The main purpose of this paper is to show that this potential may also be profitably used for the calculation of ground-state properties of doubly closed nuclei. To this end, we have employed the Goldstone expansion which, given the smooth behavior of  $V_{\text{low-k}}$ , does not require any rearrangement. As a first step of our procedure, we solve the Hartree-Fock (HF) equations for  $V_{\text{low-k}}$ . Then, using the obtained self-consistent field as auxiliary potential, we calculate the Goldstone expansion including diagrams up to third order in  $V_{\text{low-k}}$ .

Here, we present the results obtained for  $^{16}\text{O}$  and  $^{40}\text{Ca}$  starting from the new realistic  $NN$  potential of Entem and Machleidt [4] based on chiral perturbation theory at the next-to-next-to-next-to-leading order ( $N^3\text{LO}$ ; fourth order). This potential is an improved version of the earlier chiral  $NN$  potential [18] (known as Idaho potential) constructed by the same authors, which includes two-pion exchange contributions only up to chiral order 3. We have recently employed the latter potential in shell-model calculations for various two-particle valence nuclei [16].

The paper is organized as follows. In Sec. II we first describe the main features of the derivation of  $V_{\text{low-k}}$ , then outline the essentials of our calculation. In Sec. III we present our results and compare them with the experimental data. Some concluding remarks are given in Sec. IV.

**II. METHOD OF CALCULATION**

The first step in our approach is to integrate out the high-momentum components of  $V_{NN}$ . According to the general

FIG. 1. Behavior of  $E_{\text{HF}}$  with  $\hbar\omega$  and  $N$  for  $^{16}\text{O}$ .

definition of a renormalization group transformation, the decimation must be such that the low-energy observables calculated in the full theory are preserved exactly by the effective theory. Once the relevant low-energy modes are identified, all remaining modes or states have to be integrated out.

For the nucleon-nucleon problem in vacuum, we require that the deuteron binding energy, low-energy phase shifts, and low-momentum half-on-shell  $T$  matrix calculated from  $V_{NN}$  must be reproduced by  $V_{\text{low-k}}$ .

The full-space Schrödinger equation may be written as

$$H\Psi_{\mu} = E_{\mu}\Psi_{\mu}; \quad H = H_0 + V_{NN}, \quad (1)$$

where  $H_0$  is the unperturbed Hamiltonian, namely, the kinetic energy. The above equation can be reduced to a model-space one of the form

$$PH_{\text{eff}}P\Psi_{\mu} = E_{\mu}P\Psi_{\mu}, \quad H_{\text{eff}} = H_0 + V_{\text{low-k}}, \quad (2)$$

where  $P$  denotes the model space, which is defined by momentum  $k \leq k_{\text{cut}} = \Lambda$ ,  $k$  being the relative momentum and  $k_{\text{cut}}$  a cutoff momentum.

The half-on-shell  $T$  matrix of  $V_{NN}$  is

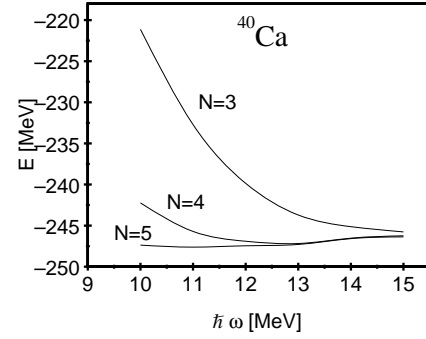
$$T(k', k, k^2) = V_{NN}(k', k) + \int_0^{\infty} q^2 dq V_{NN}(k', q) \frac{1}{k^2 - q^2 + i0^+} T(q, k, k^2), \quad (3)$$

and the effective low-momentum  $T$  matrix is defined by

$$T_{\text{low-k}}(p', p, p^2) = V_{\text{low-k}}(p', p) + \int_0^{\Lambda} q^2 dq V_{\text{low-k}}(p', q) \frac{1}{p^2 - q^2 + i0^+} \times T_{\text{low-k}}(q, p, p^2). \quad (4)$$

Note that for  $T_{\text{low-k}}$  the intermediate states are integrated up to  $\Lambda$ .

It is required that, for  $p$  and  $p'$  both belonging to  $P$  ( $p, p' \leq \Lambda$ ),  $T(p', p, p^2) = T_{\text{low-k}}(p', p, p^2)$ . In Refs. [13,14] it has been shown that the above requirements are satisfied when  $V_{\text{low-k}}$  is given by the folded-diagram series

FIG. 2. Behavior of  $E_{\text{HF}}$  with  $\hbar\omega$  and  $N$  for  $^{40}\text{Ca}$ .

$$V_{\text{low-k}} = \hat{Q} - \hat{Q}' \int \hat{Q} + \hat{Q}' \int \hat{Q} \int \hat{Q} - \hat{Q}' \int \hat{Q} \int \hat{Q} \int \hat{Q} + \dots, \quad (5)$$

where  $\hat{Q}$  is an irreducible vertex function, in the sense that its intermediate states must be outside the model space  $P$ . The integral sign represents a generalized folding operation [19], and  $\hat{Q}'$  is obtained from  $\hat{Q}$  by removing terms of first order in the interaction.

The above  $V_{\text{low-k}}$  can be calculated by means of iterative techniques. We have used here an iteration method proposed in Ref. [20], which is particularly suitable for nondegenerate model spaces. This method, which we refer to as Andreozzi-Lee-Suzuki method, is an iterative method of the Lee-Suzuki type, which converges to the lowest  $d$  eigenvalues of  $H$ ,  $d$  being the dimension of the  $P$  space. Since the  $V_{\text{low-k}}$  obtained by this technique is non-Hermitian, we have made use of the simple and numerically convenient Hermitization procedure suggested in Ref. [20]. We have verified that the deuteron binding energy and the phase shifts up to the cutoff momentum  $\Lambda$  are preserved by  $V_{\text{low-k}}$ .

An important question in our approach is what value one should use for the cutoff momentum. A discussion of this point as well as a criterion for the choice of  $\Lambda$  can be found in Ref. [14]. According to this criterion, we have used here  $\Lambda = 2.1 \text{ fm}^{-1}$ . We have found it appropriate, however, to check on the sensitivity of our results to moderate changes in the value of  $\Lambda$ . It has turned out that they change very little when letting  $\Lambda$  vary from 2.0 to 2.2  $\text{fm}^{-1}$ . For instance, at the second order in the Goldstone expansion (see the following section), the binding energy per nucleon for  $^{16}\text{O}$  is 7.29 and 7.12 MeV for  $\Lambda = 2.0$  and  $\Lambda = 2.2 \text{ fm}^{-1}$ , respectively.

As already mentioned in the Introduction, our starting point is the  $N^3\text{LO}$  potential [4]. From this potential we derive the corresponding  $V_{\text{low-k}}$  and use it directly in a HF calculation. The HF equations are then solved for  $^{16}\text{O}$  and  $^{40}\text{Ca}$  making use of a harmonic-oscillator basis. We assume spherical symmetry, which implies that the HF SP states  $|\alpha\rangle$  have good orbital and total angular momentum. Therefore, they can be expanded in terms of oscillator wave functions  $|\mu\rangle$ ,

$$|\alpha\rangle = \sum_{\mu} C_{\mu}^{\alpha} |\mu\rangle, \quad (6)$$

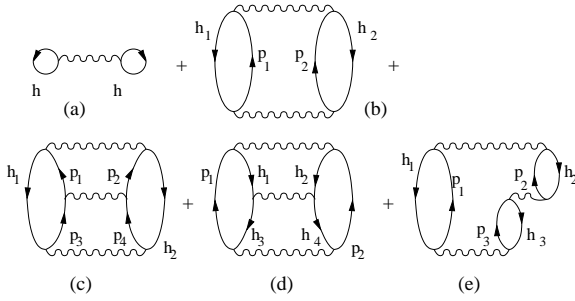


FIG. 3. First-, second-, and third-order diagrams in the Goldstone expansion.

where the sum is over the principal quantum number only. The expansion coefficients  $C_\mu^\alpha$  are determined by solving self-consistently the HF equations

$$\sum_{\mu'} \langle \mu | t + U | \mu' \rangle C_{\mu'}^\alpha = \epsilon_\alpha C_\mu^\alpha, \quad (7)$$

where  $t$  is the kinetic energy and the HF potential  $U$  is defined as

$$\langle \mu | U | \mu' \rangle = \sum_{\alpha_h} \langle \mu \alpha_h | V_{\text{low-k}} | \mu' \alpha_h \rangle, \quad (8)$$

with the index  $\alpha_h$  referring to occupied states in the ground-state HF Slater determinant.

Once Eq. (7) has been solved, the ground-state properties of the nucleus can be calculated. In particular, the total energy has the well-known expression

$$E_{\text{HF}} = \frac{1}{2} \sum_{\alpha_h} [\langle \alpha_h | t | \alpha_h \rangle + \epsilon_{\alpha_h}]. \quad (9)$$

In our calculations the sum in expansion (6) has been extended up to  $N=5$  terms. We have verified that this truncation is sufficient to ensure that the HF results do not significantly depend on the variation of the oscillator constant  $\hbar\omega$ . This is illustrated in Figs. 1 and 2, where we show the behavior of the HF ground-state energy of  $^{16}\text{O}$  and  $^{40}\text{Ca}$  versus  $\hbar\omega$  for different values of  $N$ . The results for  $N=5$  are quite stable. In our calculations the values of  $\hbar\omega$  have been derived from the expression  $\hbar\omega = 45A^{-1/3} - 25A^{-2/3}$  [21],

TABLE I. Comparison of the calculated binding energy per nucleon (MeV/nucleon) and rms charge radius (fm) with the experimental data for  $^{16}\text{O}$  and  $^{40}\text{Ca}$ .

Nucleus	HF	HF+2nd	HF+2nd +3rd	Expt.
$^{16}\text{O}$	$B/A$	3.23	7.22	7.98
	$\langle r_c \rangle$	2.30	2.52	$2.73 \pm 0.02$
$^{40}\text{Ca}$	$B/A$	6.19	9.10	8.55
	$\langle r_c \rangle$	2.610	3.302	$3.444 \pm 0.003$

TABLE II. Calculated and experimental single-particle energies (MeV) for  $^{16}\text{O}$ . Experimental data are taken from Refs. [23,26,27].

Orbital	$^{16}\text{O}$			
	Neutron		Proton	
	Calc.	Expt.	Calc.	Expt.
$s_{1/2}$	-53.786	-47	-48.606	$-44 \pm 7$
$p_{3/2}$	-23.225	-21.839	-19.264	-18.451
$p_{1/2}$	-15.649	-15.663	-11.841	-12.127
$d_{5/2}$	-0.056	-4.144	3.564	-0.601
$s_{1/2}$	-0.481	-3.273	2.651	-0.106
$d_{3/2}$	5.814	0.941	8.713	4.399

which reproduces the rms radii in an independent-particle approximation with harmonic-oscillator wave functions. This expression gives  $\hbar\omega = 14$  and 11 MeV for  $^{16}\text{O}$  and  $^{40}\text{Ca}$ , respectively. In solving Eq. (7), the Coulomb potential has been added to  $V_{\text{low-k}}$  for protons.

We use the HF basis to sum the Goldstone expansion including contributions up to third order in  $V_{\text{low-k}}$ . In Fig. 3 we report the first-, second-, and third-order diagrams [22]. The intermediate states involved in the evaluation of these diagrams are those obtained from the lowest 10 and 11 harmonic-oscillator major shells for  $^{16}\text{O}$  and  $^{40}\text{Ca}$ , respectively. Our results show convergence for these large spaces: for example, the  $^{16}\text{O}$  binding energy per nucleon in second-order approximation is 7.03, 7.22, and 7.30 MeV when considering 9, 10, and 11 major shells, respectively. Similar diagrams have been used to calculate the corrections to the rms radius. As is well known, retaining only the first-order term in this expansion yields the HF results.

To conclude, it is worth stressing that using the Goldstone expansion in terms of  $V_{\text{low-k}}$  one has to include also diagrams (b) and (c). This is not the case of the BG approach, where

TABLE III. Calculated and experimental single-particle energies (MeV) for  $^{40}\text{Ca}$ . Experimental data are taken from Refs. [23,26,27].

Orbital	$^{40}\text{Ca}$			
	Neutron		Proton	
	Calc.	Expt.	Calc.	Expt.
$s_{1/2}$	-97.944		-87.501	$-49.1 \pm 12$
$p_{3/2}$	-63.760		-53.934	$-77 \pm 14$
$p_{1/2}$	-54.959		-45.269	$-33.3 \pm 6.5$
$d_{5/2}$	-33.018	-21.30	-23.749	$-32 \pm 4$
$s_{1/2}$	-27.406	-18.104	-18.238	$-14.9 \pm 2.5$
$d_{3/2}$	-19.595	-15.641	-10.663	$-13.8 \pm 7.5$
$f_{7/2}$	-6.579	-8.363	2.047	-10.850
$p_{3/2}$	-4.325	-6.420	3.293	-8.328
$p_{1/2}$	-0.973		5.865	-1.085
$f_{5/2}$	5.852		12.484	0.631

TABLE IV. Calculated occupation probabilities for  $^{16}\text{O}$ .

Orbital	Proton	Neutron
$s_{1/2}$	0.881	0.881
$p_{3/2}$	0.822	0.818
$p_{1/2}$	0.767	0.760

these diagrams are already contained in diagram (a) through the  $G$  matrix.

### III. RESULTS

In Table I, the calculated binding energy per nucleon and the rms charge radius for both  $^{16}\text{O}$  and  $^{40}\text{Ca}$  are compared with the experimental data [23–25]. This table contains the HF results as well as the values obtained including second- and third-order contributions. We see that the renormalization of the short-range repulsion through  $V_{\text{low-k}}$  is sufficient to yield positive HF binding energies, albeit too small as compared to the experimental values. We also see that the HF approximation significantly underestimates the rms radii. This evidences the role of higher-order contributions in the Goldstone expansion to account for correlations beyond the mean field. The binding energies and radii calculated including diagrams up to third order are very satisfactory. In fact, the binding energies gain about 4 and 3 MeV for  $^{16}\text{O}$  and  $^{40}\text{Ca}$ , respectively, while the radii increase by about 0.4 and 0.8 fm coming quite close to the experimental values.

A discussion of the convergence properties of the perturbative series is now in order. To this end, the HF potential energy, the second-order, and third-order corrections have to be compared. In  $^{16}\text{O}$  the HF potential energy per nucleon is  $V^{(1)} = -23.5$  MeV, which is obtained by subtracting from the total HF energy the contribution of the kinetic term. Thus for the ratio of the second- to first-order term we obtain  $V^{(2)}/V^{(1)} = 0.17$ , while the ratio  $V^{(3)}/V^{(2)}$  is 0.08. Similarly, for  $^{40}\text{Ca}$  we have  $V^{(1)} = -33.7$  MeV,  $V^{(2)}/V^{(1)} = 0.09$ , and  $V^{(3)}/V^{(2)} = 0.03$ . On these grounds, we may conclude that the convergence of the series is fairly rapid and that higher-order contributions are negligible.

For the sake of completeness, in Tables II and III we report the HF single-hole energies as well as the energies of the low-lying particle states of  $^{16}\text{O}$  and  $^{40}\text{Ca}$ . In Tables IV and V the calculated occupation probabilities for states up to the Fermi level are reported.

### IV. CONCLUDING REMARKS

In this work, starting from the chiral  $\text{N}^3\text{LO}$  potential [4], we have performed calculations for the ground-state properties of the doubly closed nuclei  $^{16}\text{O}$  and  $^{40}\text{Ca}$  making use of

TABLE V. Calculated occupation probabilities for  $^{40}\text{Ca}$ .

Orbital	Proton	Neutron
$s_{1/2}$	0.945	0.947
$p_{3/2}$	0.931	0.932
$p_{1/2}$	0.921	0.922
$d_{5/2}$	0.885	0.884
$s_{1/2}$	0.858	0.855
$d_{3/2}$	0.811	0.807

the Goldstone expansion. This has been done within the framework of a new approach [13,14] to the renormalization of the short-range repulsion of realistic  $NN$  potentials, wherein a low-momentum potential  $V_{\text{low-k}}$  is constructed which preserves the low-energy physics of the original potential. We consider a main achievement of our study to have shown that  $V_{\text{low-k}}$  is suitable for being used directly in the Goldstone expansion. Namely, unlike the traditional BHF approach, there is no need to first calculate the  $G$  matrix. We have seen that taking into account higher-order contributions (essentially the second-order terms) of  $V_{\text{low-k}}$  in the Goldstone expansion yields very good results for the binding energy and charge radius of  $^{16}\text{O}$  and  $^{40}\text{Ca}$ .

In this context, it is worth emphasizing that the idea of bypassing the  $G$ -matrix approach to nuclear structure calculations is not new [28,29]. From this viewpoint, the present study comes close in spirit to the early work carried out at the MIT [30–32] in the mid 1960s. There Tabakin’s separable nonlocal  $NN$  potential [28] was used in HF calculations and then the second-order correction to the binding energy was evaluated, obtaining quite satisfactory results. It is indeed very gratifying that our results based on the use of the  $V_{\text{low-k}}$  derived from the modern  $\text{N}^3\text{LO}$  potential come significantly closer to the experimental data. It should be noted that our results are quite good also when compared to those of recent BHF calculations [8], where different modern  $NN$  potentials have been used and long-range correlations have been considered within the framework of the Green function approach.

In summary, we may conclude that the results of the present study, together with those of our recent shell-model calculations, show that the  $V_{\text{low-k}}$  approach provides a simple and reliable way of “smoothing out” the repulsive core contained in the modern  $NN$  potentials before using them in microscopic nuclear structure calculations.

### ACKNOWLEDGMENTS

This work was supported in part by the Italian Ministero dell’Istruzione, dell’Università e della Ricerca (MIUR) and by the U.S. Department of Energy Grant No. DE-FG02-88ER40388. We would like to thank R. Machleidt for providing us with the matrix elements of the  $\text{N}^3\text{LO}$  potential.

[1] R. Machleidt, Phys. Rev. C **63**, 024001 (2001).

[2] V.G.J. Stoks, R.A.M. Klomp, C.P.F. Terheggen, and J.J. de

Swart, Phys. Rev. C **49**, 2950 (1994).

[3] R.B. Wiringa, V.G.J. Stoks, and R. Schiavilla, Phys. Rev. C **51**,

- 38 (1995).
- [4] D.R. Entem and R. Machleidt, nucl-th/0304018.
- [5] See, for instance, B.D. Day, Rev. Mod. Phys. **39**, 719 (1967).
- [6] I. S. Towner, *A Shell Model Description of Light Nuclei* (Clarendon, Oxford, 1977).
- [7] K.W. Schmid, H. Mütter, and R. Machleidt, Nucl. Phys. **A530**, 14 (1991), and references therein.
- [8] Kh. Gad and H. Mütter, Phys. Rev. C **66**, 044301 (2002).
- [9] A. Fabrocini, F. Arias de Saavedra, and G. C6, Phys. Rev. C **61**, 044302 (2000), and references therein.
- [10] Jochen H. Heisenberg and Bogdan Mihaila, Phys. Rev. C **59**, 1440 (1999), and references therein.
- [11] H. Mütter and A. Polls, Prog. Part. Nucl. Phys. **45**, 243 (2000).
- [12] K. Suzuki and R. Okamoto, Prog. Theor. Phys. **92**, 1045 (1994).
- [13] S. Bogner, T.T.S. Kuo, and L. Coraggio, Nucl. Phys. **A684**, 432c (2001).
- [14] Scott Bogner, T.T.S. Kuo, L. Coraggio, A. Covello, and N. Itaco, Phys. Rev. C **65**, 051301(R) (2002).
- [15] A. Covello, L. Coraggio, A. Gargano, N. Itaco, and T. T. S. Kuo, in *Challenges of Nuclear Structure*, Proceedings of the Seventh International Spring Seminar on Nuclear Physics, Maiori, Italy, 2001, edited by A. Covello (World Scientific, Singapore, 2002), p. 139.
- [16] L. Coraggio, A. Covello, A. Gargano, N. Itaco, T.T.S. Kuo, D.R. Entem, and R. Machleidt, Phys. Rev. C **66**, 021303(R) (2002).
- [17] L. Coraggio, A. Covello, A. Gargano, N. Itaco, and T.T.S. Kuo, Phys. Rev. C **66**, 064311 (2002).
- [18] D.R. Entem and R. Machleidt, Phys. Lett. B **524**, 93 (2002); D.R. Entem, R. Machleidt, and H. Witala, Phys. Rev. C **65**, 064005 (2002).
- [19] E.M. Krenciglowa and T.T.S. Kuo, Nucl. Phys. **A342**, 454 (1980).
- [20] F. Andreozzi, Phys. Rev. C **54**, 684 (1996).
- [21] J. Blomqvist and A. Molinari, Nucl. Phys. **A106**, 545 (1968).
- [22] J. Goldstone, Proc. R. Soc. London, Ser. A **239**, 267 (1957).
- [23] G. Audi and A.H. Wapstra, Nucl. Phys. **A565**, 1 (1993).
- [24] H. de Vries, C.W. de Jager, and C. de Vries, At. Data Nucl. Data Tables **36**, 495 (1987).
- [25] E.G. Nadjakov, K.P. Marinova, and Yu.P. Gangrsky, At. Data Nucl. Data Tables **56**, 133 (1994).
- [26] Data extracted using the NNDC On-Line Data Service from the ENSDF database, files revised as of December 5, 2001, M. R. Bhat, *Evaluated Nuclear Structure Data File (ENSDF), Nuclear Data for Science and Technology*, edited by S. M. Quaim (Springer-Verlag, Berlin, Germany, 1992), p. 817.
- [27] M.A.K. Lodhi and B.T. Waak, Phys. Rev. Lett. **33**, 431 (1974).
- [28] F. Tabakin, Ann. Phys. (N.Y.) **30**, 51 (1964); Phys. Rev. **174**, 1208 (1968).
- [29] J.P. Elliott, A.D. Jackson, H.A. Mavromatis, E.A. Sanderson, and B. Singh, Nucl. Phys. **A121**, 241 (1968).
- [30] A.K. Kerman, J.P. Svenne, and F.M.H. Villars, Phys. Rev. **147**, 710 (1966).
- [31] A.K. Kerman and M.K. Pal, Phys. Rev. **162**, 970 (1967).
- [32] W.H. Bassichis, A.K. Kerman, and J.P. Svenne, Phys. Rev. **160**, 746 (1967).